

Postdiction of the Flexural Shear Capacity of a Deep Beam Without Stirrups Using NLFEM

Yang, Yuguang; de Boer, Ane; den Uijl, Joop

DOI

[10.1080/10168664.2021.1894631](https://doi.org/10.1080/10168664.2021.1894631)

Publication date

2021

Document Version

Accepted author manuscript

Published in

Structural Engineering International

Citation (APA)

Yang, Y., de Boer, A., & den Uijl, J. (2021). Postdiction of the Flexural Shear Capacity of a Deep Beam Without Stirrups Using NLFEM. *Structural Engineering International*, 31(2), 208-215.
<https://doi.org/10.1080/10168664.2021.1894631>

Important note

To cite this publication, please use the final published version (if applicable).
Please check the document version above.

Copyright

Other than for strictly personal use, it is not permitted to download, forward or distribute the text or part of it, without the consent of the author(s) and/or copyright holder(s), unless the work is under an open content license such as Creative Commons.

Takedown policy

Please contact us and provide details if you believe this document breaches copyrights.
We will remove access to the work immediately and investigate your claim.



44

45 Scientific Paper

46 Submitted date: [Click here to enter Date.](#)

47 Postdiction of the flexural shear capacity of a 48 deep beam without stirrups using NLFEM

49 Yuguang Yang¹, Ane de Boer², Joop den Uijl³

50 ¹ Delft University of Technology, Delft, the Netherlands

51 ² Ane de Boer Consultancy, Arnhem, the Netherlands

52 ³ Delft University of Technology, Delft, the Netherlands

53 Abstract

54 A recent contest of shear tests modelling was carried out in 2019. Teams from universities and consultancies
55 around Europe were invited to predict the shear capacity of two reinforced concrete beams. The basics of the
56 numerical models should be setup according the Dutch NLFEM Guideline RTD 1016-1:2017. In the contest, two
57 reinforced concrete beams without stirrups but with a large depth (1200 mm) tested at Delft University of
58 Technology were selected as modelling target. Most participants of the contest did not get good agreement with
59 the test results. This paper presents a postdiction study on one of the two tests: H123. Based on this study, some
60 adaptations are made to the recommendations of RTD 1016-1:2017 in order to better approach the test results.
61 The intention of this contribution is to improve the existing NLFEM Guideline for practical engineering structures
62 with uncommon reinforcement layout.

63 **Keywords:** reinforced concrete, shear failure, deep beam, without shear reinforcement, NLFEM

64 Introduction

65 Application of smeared cracking approach based Non-Linear Finite Element Method (NLFEM) is becoming
66 more accepted in the engineering practice to model the nonlinear behaviour of structural concrete with
67 complex loading conditions and geometries. Nowadays, general design provisions for structural concrete
68 members such as Eurocode (CEN, 2005) and Model Code 2010 (fib, 2012) specify that the resistance of
69 structural concrete members can be evaluated using NLFEM when simplified analytical approach may not
70 provide an estimation with sufficient accuracy. However, modelling with NLFEM was shown to be sensitive to
71 the choices of the modelling techniques and parameters (Belletti, et al., 2010). And it becomes time consuming
72 if one needs many trials to get a reliable simulation. With the intension of simplifying the modelling process for
73 engineering application, the Dutch Ministry of Infrastructure and Water Management (Rijkswaterstaat)
74 provided a Guideline for Nonlinear Finite Element Analysis of Concrete Structures RTD 1016-1:2017
75 (Rijkswaterstaat, 2017a), which deals with the modelling of concrete structures using smeared cracking based
76 NLFEM. The intension of the guideline is provide a simple general modelling approach, which will yield reliable
77 and conservative predictions without significantly losing accuracy compared to more tailored NLFEM models.

78

79 To gain experience and build up confidence on RTD 1016-1, several validation studies on well documented
80 experiments have been published in RTD1016-2, 3A, 3B, 3C (Rijkswaterstaat, 2017b), covering three types of
81 structures, namely reinforced concrete beams, prestressed beams and slabs. In addition to that, two
82 international contests based on unpublished experiments have been organized by the User Association of
83 DIANA (Ensink, et al., 2015; Yang, et al., 2021b). The participants are from research institutes and engineering
84 companies who use NLFEM and are familiar with RTD 1016-1. Its recent edition, in 2019, aimed at the
85 simulation of two shear tests on reinforced concrete beams without shear reinforcement carried out at Delft
86 University of Technology. The specimens were selected from a large research program on shear behaviour of

87 RC slab strips (Yang, et al., 2021b). The original goal of the research program was to investigate the size effect
88 on the shear capacity of existing RC slab bridges without shear reinforcement.

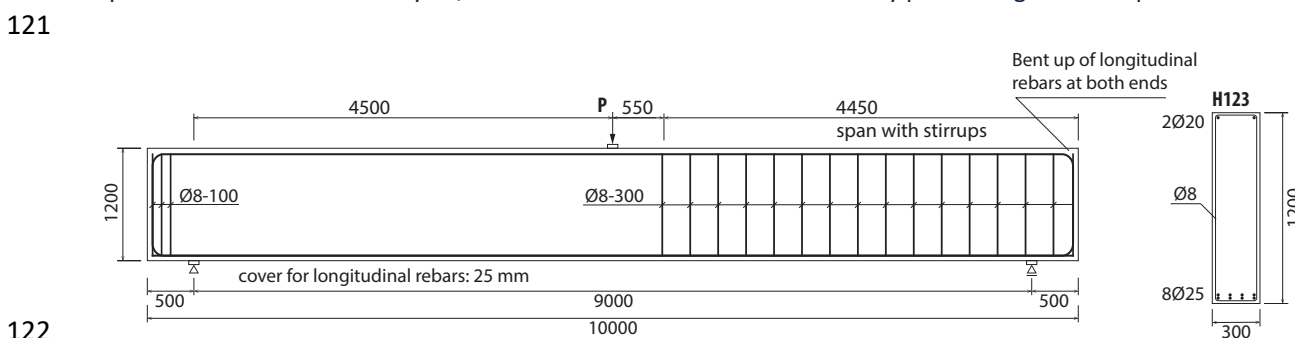
89
90 In the contest, two unpublished shear tests on RC beams (slab strips) with 1200 mm depth were selected. The
91 participants were asked to predict the shear capacity of these beams with any approach including numerical
92 and analytical models. When NLFEM would be applied, it was advised to follow RTD 1016-1 (but this was not
93 compulsory). The provided information before the competition included the detailed geometry of the
94 specimen, the reinforcement configurations, the test setup and the mechanical properties of concrete and
95 reinforcement (also listed in Table 1). The results of the simulations were disappointing, despite that most
96 contributions followed the aforementioned design codes and guidelines. On average, an overestimation of
97 more than 140 % of the experimental capacity was obtained from the total 10 contributions submitted to the
98 contest. A summary of the contest and the results was reported in (Yang, et al., 2021b; Yang, et al., 2021b). To
99 the owners of existing large infrastructural structures, like Rijkswaterstaat, the contest results might raise the
100 following question:

101
102 *Is RTD 1016-1 still reliable, and how should RTD 1016-1 be improved with the obtained information?*

103
104 Out of the two beams in the contest: H123 ($\rho_l = 1.14\%$) and H352 ($\rho_l = 0.36\%$), H123 was selected in the
105 present study considering that it had a more practical longitudinal reinforcement ratio. With the test results
106 known, this paper focuses on searching for an improved set of choices based on a postdiction study. As for
107 NLFEM, in addition to the loading conditions and the material properties, the choices of modelling parameters
108 and solution strategies may affect the simulation results as well. The intention of the present study is to
109 investigate the possibility of approaching the test results by adjusting these parameters and demonstrate a
110 step-by-step approach of improving the modelling flexural shear failure of deep RC members without shear
111 reinforcement. The study is mainly based on the commercially available NLFEM software package DIANA, to
112 avoid bias another software package ATENA is used in an additional validation case.

113 Shear test on beam H123

114 The shear test H123 was designed to investigate the size effect of a realistic configured RC member without
115 shear reinforcement. The dimensions and the reinforcement configurations of the test specimen are given in
116 Figure 1. As shown, the specimen was loaded by a single point load at mid-span, with the left side being
117 considered as test span. Half of the longitudinal reinforcement bars were bent up to the top side of the
118 specimen with the other half welded at the bar ends to the bent-up bars, in order to ensure sufficient
119 anchorage at the beam ends. The reinforcement bars were arranged in two layers, however no spacing was
120 specified between the two layers, which were connected to each other by pit welding at a few spots.



122
123 **Figure 1. Dimensions, test conditions and reinforcement configurations of H123.**

124
125 At the date of the experiment, several material properties were tested in the lab using concrete cubes of 150
126 mm. The average values of these properties, which were given to the participants of the contest, are shown in
127 Table 1. In the contest, it depended on the users' interpretation for the input in their NLFEM simulations based
128 on this information.

129

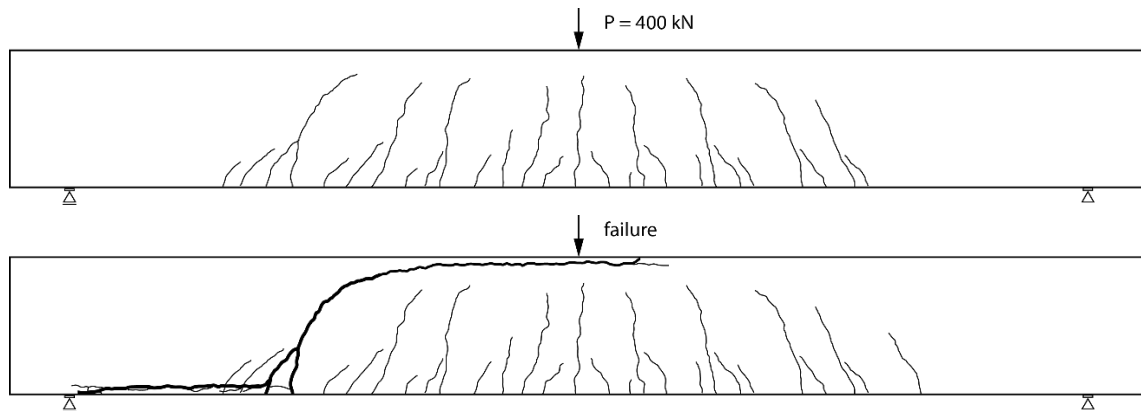


130 **Table 1. Material parameters obtained from lab tests.**

Parameter		value	units
Concrete strength (from 150 mm cube tests)	$f_{c,cube}$	86.9	MPa
Concrete tensile strength (from splitting tests of 150 mm cubes)	$f_{ct,split}$	5.7	MPa
Maximum aggregate size	d_a	16	mm
Density of concrete	ρ_c	23.9	kN/m ³
Yield stress reinforcement	f_{yk}	583.9	MPa
Ultimate stress reinforcement	f_{ik}	683.9	MPa

131

132 In the test, the beam failed at a maximum load of 445 kN. The crack patterns of the specimen at $P = 400$ kN
133 and after the formation of the flexural shear crack are shown in Figure 2. As indicated by the crack pattern at
134 400 kN and 445 kN, the critical shear crack initiated from the last flexural crack. Further propagation of the
135 flexural shear crack resulted in failure of the specimen. The observed crack pattern is utilized for comparison
136 with the output of the simulation results.



137 **Figure 2. Crack pattern of H123 at the last load level before failure (top figure) and the crack pattern after failure**
138 **(bottom figure).**

139

140 In the test, the critical shear crack formed from the already present flexural crack at 400 kN. At the
141 peak load, two secondary cracks developed from one of the major flexural cracks into the
142 compression zone and along the longitudinal reinforcement. The propagation process of these two
143 branches was very unstable, which leads to the sudden drop of the bearing capacity and the increase
144 of the deflection. This type of failure is typically defined as flexural shear failure as suggested by
145 (Yang, 2014). The unstable propagation of the flexural shear crack at failure leads to a drastic change
146 of the deformation and stress distribution in the whole beam. This is usually difficult to be captured
147 by numerical models without lack of convergency.

148 **Modelling choices based on the RTD 1016-1 guideline**

149 In addition to the information provided by the call of the contest (shown in Table 1), the missing parameters
150 for the NLFEM are obtained following the instructions of RTD1016-1, which leads to the additional material
151 and analysis parameters given in Table 2.

152

153 Out of the listed parameters, this study will first discuss the choices of the concrete parameters which are not
154 always directly reflected by lab specimen tests, such as the concrete tensile strength f_{ctm} . Next, the study
155 discusses the influences of the modelling choices and analysis parameters to the simulation results. These
156 parameters includes: rotating/fixed crack model, element size and bond-slip model. After comparing with the

157 test results, further improvements of the modelling choices and analysis parameters that do not relate to the
158 material properties are made.

159

160 **Table 2. Additional material and nonlinear analysis parameters**

Parameter	Value
f_{cm}	71.2 MPa
G_f	157.3 N/m
G_c	250× G_f
Poisson ratio	0.15
Crack model	rotated
f_{ctm}	4.44 MPa
Young's modulus	39.2 GPa
Convergence	Energy + Force
Element size over height girder	100 mm (Mapped mesh)
Arclength	Regula
Model of Reinforcement	Bar element
Bonded/bond slip	Perfect bond

161

162 Regarding the concrete tensile strength, in the announcement of the contest, the tensile strength of the
163 concrete was reported to be 5.7 MPa, which was obtained by splitting tensile tests. However, the direct tensile
164 strength f_{ctm} should be used when analysing the tensile behaviour of concrete in a NLFEM. This is also
165 recommended by RTD1016-1 and other design codes such as the *fib* Model Code 2010. In this study the
166 concrete tensile strength f_{ctm} is directly derived from the concrete compressive strength.

167

168 The validation studies reported by (Rijkswaterstaat, 2017c), suggest to apply the total strain rotating crack
169 model as the default choice of the material model. As demonstrated by (Rots, 1989), the rotating crack model
170 turns out to be more robust against shear locking, thus it typically provides a lower prediction than the fixed
171 crack model type. For engineering practice, the ease of use of the rotating crack model combined with its
172 conservative prediction is considered as great benefit. Thus in RTD 1016-1 rotating crack model is suggested.
173 However, as suggested in (Yang, et al., 2017) the shear capacity of RC members without shear reinforcement
174 may be affected by the crack pattern, while rotating crack model is known not to be able to accurately
175 simulate the crack pattern. In the study, both the rotating crack model and the fixed crack model are therefore
176 employed. Following the default settings of the software, the rotating crack model is typically used in DIANA
177 and the fixed crack model in ATENA.

178

179 In terms of element size, mesh sensitivity study is generally recommended by most NLFEM packages (DIANA
180 FEA, 2020; Cervenka & Jendele, 2009) as well as design codes (fib, 2012). Although with the introduction of the
181 crack band theory proposed by (Bažant & Oh, 1983), the effect of element size on the cracking behaviour of
182 concrete is taken into account for models with regular mesh layout. For shear simulations, recent studies
183 reported by (Slobbe, et al., 2013) and (Cervenka, et al., 2016) showed that the element size and orientation
184 still have a clear influence on the prediction results. Therefore, the influence of element size is chosen as a
185 modelling parameter to be studied in this paper. RTD 1016-1 suggests a maximum element size of $h/6$ over the
186 height of the beam. It is expected that a smaller element size will lead to more accurate prediction. Thus to
187 simulate the H123 beam with a height of 1200 mm, a larger number of elements (more than 6 elements) over
188 the height of the beam is foreseen. In (Červenka, et al., 2018), the maximum element size for members with
189 tensile cracking is suggested to be the expected crack spacing. The minimum element size was not introduced
190 yet in RTD 1016-1 in 2017. In (Bažant, et al., 1984; Červenka, et al., 2018) the minimum element size was
191 suggested to be 1.5 – 3 times the maximum aggregate size in order to fulfil the basic assumption of local
192 continuum theory.

193



194 The third study parameter is the bond-slip model of the reinforcement bars. In RTD 1016-1, a reinforcing bar is
195 modelled by embedded elements with perfect bond to concrete. It means that when the tensile strain of the
196 reinforcement becomes larger than the cracking strain of concrete, the concrete elements crack in order to
197 fulfil the kinematics conditions. The introduction of a bond-slip model when modelling the embedded
198 reinforcement leads to a more realistic crack pattern at the level of the tensile reinforcement. This is
199 considered as an option to provide a more accurate prediction to model failure modes which are sensitive to
200 the crack propagation like the H123 beam. In this study the bond-slip model proposed by (Shima, et al., 1987)
201 is selected in the reference model. The model describes the interaction between a reinforcing bar and the
202 surrounding concrete at macro level. In this model reduction of bond stress due to local failure of the interface
203 is not considered. Thus it needs only an input value for the compression strength. The bond-slip model of
204 Shima is adapted in some of the DIANA models. The bond-slip model of the MC2010 (fib, 2012), on the other
205 hand, takes into account different bond failure modes (pull-out and splitting), which results in different bond
206 stress-slip relations. With the bond-slip model suggested by Model Code 2010, the unloading of the bond
207 stress due to local failure under large slip can be modelled as well. The Model Code 2010 bond-slip model is
208 adapted in the ATENA model (Jendele & Cervenka, 2006) presented in this study.

209
210 Beside the modelling choices of the simulation, the convergence criteria may affect the results as well. They
211 may be chosen amongst displacement, force or energy based criteria, coupling two or all three criteria. For
212 each choice, the values for the tolerance of the criteria will affect the simulation results. A recent study
213 reported in (de Putter, 2020) shows this effect. In the study, it was recommended that for simulations with
214 brittle failures like the flexural shear failure of RC members without shear reinforcement, in order to continue
215 the simulation with reasonable accuracy, it is not necessary to continue simulation steps with all the criteria
216 fulfilled. In RTD 1016-1, using the maximum values of 0.001 for the energy criterion and 0.01 for the force
217 criterion is recommended. Imposing multiple convergence criteria in a simulation often leads to unnecessary
218 load steps or even early divergence in critical load step(s). In engineering practice, in order to go over such
219 critical load step(s), a choice of relaxing the convergence criteria or reducing the number of criteria is
220 employed. In this paper, with the intention of simplifying the study, only the Energy norm (criterion) amongst
221 the other criteria is selected to study further, to be in line with RTD 1016-1.

222
223 In test H123A, the load was applied by an actuator using displacement control due to safety considerations.
224 However, most structures in engineering practice are designed for force controlled loads such as gravity, wind
225 pressure or traffic loading. Ideally NLFEM simulations loaded by either displacement or force control should
226 give comparable results. Taking that into account, in this study both loading methods are applied to the same
227 model in order to evaluate the potential difference between the two loading approaches. They are
228 distinguished by a (displacement control) or b (force control) after the simulation No. when they are referred
229 in the text.

230 Effect of element size

231 The effect of element size in the simulation is studied first in three simulations using element sizes varying
232 from 200 mm to 50 mm, which leads to 6 to 24 elements in the height of the beam. The configurations of
233 Simulations 01 – 03 are listed in Table 3. The basic modelling choices follow RTD 1016-1 and Table 2. The
234 convergence limit of Energy is set to 1.0E-4. According to RTD 1016-1, all load steps should converge till the
235 ULS is reached with a convergence value for Energy tolerance of 1.0E-3.

236

237 **Table 3. Results of element size simulations**

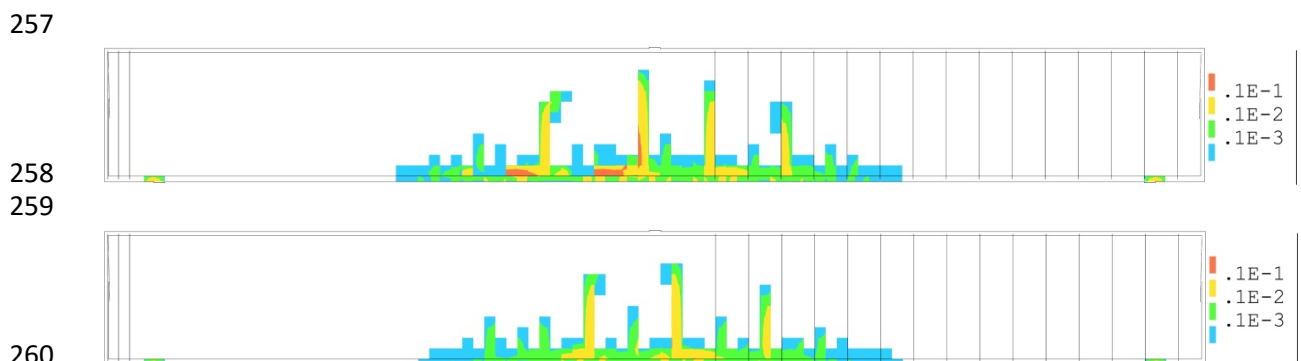
Simulation No.	Element size [mm]	$P_{max,disp}^{1)}$ [kN]	$P_{max,disp}/P_{Test}$ [-]	$P_{max,forc}^{2)}$ [kN]	$P_{max,disp}/P_{Test}$ [-]	$P_{max,forc}/P_{max,disp}$ [-]
D01	200	432	0.97	441	0.99	1.02
D02	100	365	0.82	346	0.77	0.95
D03	50	301	0.68	279	0.63	0.93

238 1) $P_{max,disp}$ is the maximum applied load before the convergence criterion was reached. In the simulation,
239 the load was applied by displacement control. Accordingly, the simulations are named as D01a –
240 D03a.

241 2) $P_{max,forc}$ is the maximum applied load before the convergence criterion was reached. In the simulation,
242 the load was applied by force control. Accordingly, the simulations are named as D01b – D03b.

243
244 Table 3 shows the results of the three simulations with different element sizes. The maximum load level of
245 Simulation D01a is close to the experimental load level. Using a finer mesh results in a reduction of the
246 ultimate load till a maximum load of 279 kN from D03b. Both smaller element models show a lower ultimate
247 load with force controlled (b series models) than with displacement controlled loading (a series models).
248 However the difference between both loading methods is rather small, at most 7.3%. Figure 3 shows the crack
249 patterns of Simulation D02 using both displacement control and force control analyses.

250
251 The results of the simulation indeed demonstrates the influence of element size upon the failure load.
252 However this conclusion is rather different from what was reported in (Cervenka, et al., 2016). In the study of
253 Cervenka et.al., models with larger element size leads to lower capacity. However, our simulations using both
254 loading methods show that by using a larger element size, higher capacity is predicted. Further study is still
255 needed to investigate the reason of the mesh dependency in both studies and the possible solutions to resolve
256 it.



260
261 **Figure 3 Crack pattern just before ULS Load level from Simulation D02a displacement controlled (top) and from**
262 **Simulation D02b force controlled (bottom).**

263
264 In terms of crack patterns, Figure 3 shows that the different loading methods give rather similar predictions,
265 with slightly different magnitude of the maximum crack strains before failure. The red and yellow coloured
266 strains show that cracks initiate along the longitudinal reinforcement. Similar cracking is reported in (de Putter,
267 2020). Further loading leads to the loss of load bearing capacity. As comparison, the crack pattern of H123 at
268 the load step before failure ($P = 400$ kN) is shown in Figure 2. The crack pattern of both methods turns out to
269 be rather comparable to the measured crack pattern, although the final crack pattern at failure cannot be
270 shown because the critical shear crack only occurred at the very last load step which leads to divergence of the
271 simulation. Most cracks before failure were flexural cracks, with which limited rotation of the crack is
272 expected. Nevertheless, at several spots at the bottom of the flexural cracks, initiation of longitudinal cracks
273 can be observed along the reinforcing bars. This observation shows that an accurate bond-slip model is needed
274 as an additional input option to get a more realistic behaviour around the reinforcement bar in order to obtain
275 a more accurate failure load.

276 Bond slip model and analysis parameters

277 In Simulation D01 – D03, no clear shear crack was observed before failure. This could also because of a too
278 relaxed convergence criterion. In order to avoid the discussions about the choice of the convergence criterion,
279 another set of simulations (Simulations D04 – D06) was developed. From Simulation D01 – D03 it was
280 concluded that an accurate bond-slip model might be a critical requisite for the simulation. Thus, the bond-slip
281 model of Shima (Shima, et al., 1987) is also introduced in the new set of simulations. The FE models have a
282 mesh with element size of 50 mm. This choice is based on the assumption that models with finer mesh size are
283 able to represent the behaviour of a structure in more detail, thus has the potential to provide better
284 accuracy. The main difference between the three simulations is the value of the energy norm. In Simulation
285 D04, the energy norm is set to 1.0E-3 as suggested by RTD 1016-1, while the other two simulations employ an
286 energy norm of 10.E-4 and 10.E-5, respectively, see Table 4. Both the displacement control and force control
287 method are used in these simulations.



288
289

Table 4. Results of analyses on convergence energy criterion, all simulations use element size of 50 mm.

Simulation No.	Energy norm	Arc length control	$P_{max,disp}$ [kN]	$P_{max,disp}/P_{Test}$ [-]	$P_{max,forc}$ [kN]	$P_{max,forc}/P_{Test}$ [-]	$P_{max,forc}/P_{max,disp}$ [-]
D04	1.0E-3	Automatic	392.3	0.88	348.5	0.78	0.89
D05	1.0E-4	Automatic	348.7	0.78	372.5	0.84	1.07
D06	1.0E-5	Automatic	378.2	0.85	364.4	0.82	0.96
D07	1.0E-4	Manual	-	-	456.9	1.03	-
D08	1.0E-5	Manual	-	-	405.9	0.91	-

290

291

292

293

294

295

296

297

298

Table 4 shows the results of the second series of simulations. Comparison of the results with the 50 mm element size simulation in table 3 and the results of table 4 yields the first conclusion that the ultimate load level is increased by implementing the bond-slip model. A second conclusion is that the load level does not change significantly when the tolerance value is increased. Both loading methods show this aspect. The difference between model predictions and test results is around 20%. Although more simulations are still needed to draw solid conclusions, one may consider that introduction of a bond-slip model may change the results of the simulations, and could provide a more reasonable estimation.

299

300

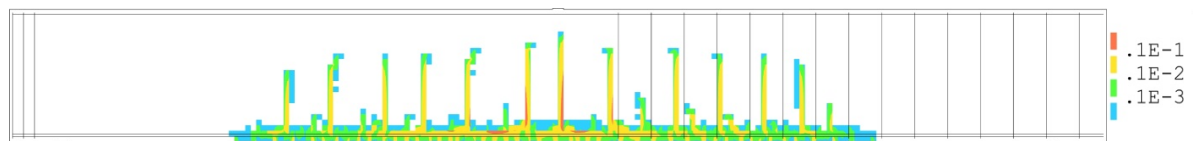
301

302

303

304

The crack pattern of Simulation D05 is shown in Figure 4. Compared to Figure 3, a more developed pattern of cracks is present by the introduction of the bond-slip model. Also the crack spacing at mid-depth of the beams turns out to be more representative to that observed in the experiments in Figure 2. Compared to the perfect bond model, a realistic bond-slip model enables the localization of crack opening amongst the elements at the rebar level, that clearly results in a more realistic crack pattern. Thus this can be seen as an improved result.



305

306

Figure 4. Overview crack pattern force controlled method for Simulation D05.

307

308

309

310

311

312

313

314

315

316

317

318

319

320

321

The ratio between the maximum load observed in the experiments (445 kN) and the simulations (348 – 392 kN) is still low. A further improvement was made by adjusting the arc length analysis. As suggested by (Verhoosel, et al., 2008), the adaption of arc length analysis may improve the stability of the analysis, thus being able to obtain the snap-back behaviour of the structure. RTD 1016-1 recommends arc length analysis to improve the convergence of the simulation. As an additional improvement, the default automatic arc length approach is replaced. In the new simulations, the control displacement is set to the bottom fibre of the left half length of the girder. Thus, the crack length of the bottom fibre of the concrete becomes more important in determining the load factor in the arc length calculation. Two new simulations are made in the additional study, Simulation D07 and D08 in table 4. Since from the previous study, the different loading approaches show very limited influence to the simulation results, in Simulation D07 – D08 only force control was applied. When comparing with the test results, the simulated ultimate load reached 90% of the experimental result and on the lower side. Hence, the adjustment of the arc length approach can be considered as a further improvement.

322

323

324

325

326

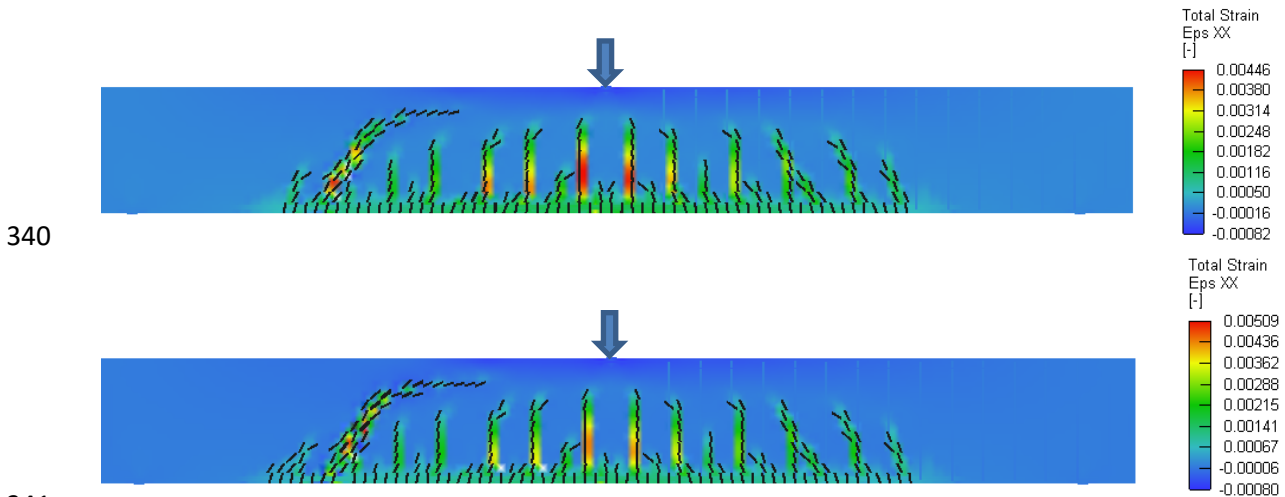
327

328

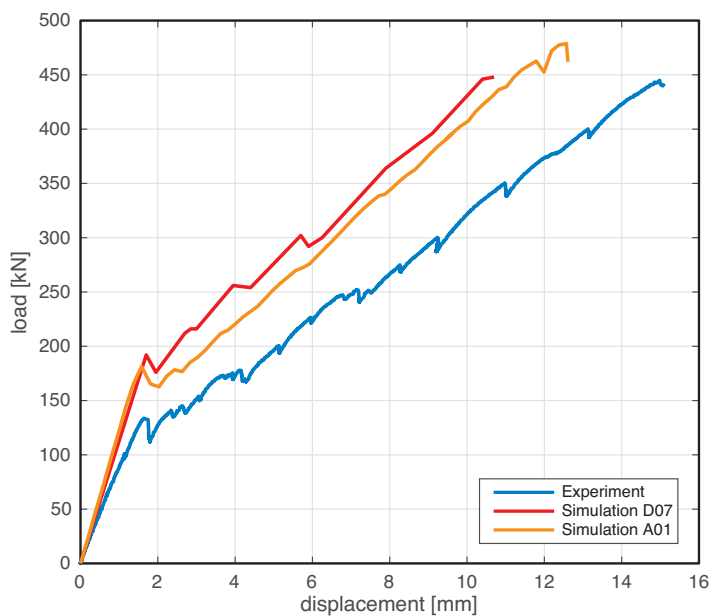
329

As was done in (Belletti, et al., 2010) and (Rijkswaterstaat, 2017b), test H123 is also simulated with the software package ATENA. Being different from the models in DIANA, the rebars in ATENA are modelled using embedded elements, but incorporated explicitly with a bond-slip model. The bond-slip model proposed in the Model Code 2010 (fib, 2012) is employed. The bond-slip model suggested in Model Code 2010 includes the softening parts of bond-slip relationship. And it can consider different bond failure modes. The model is numbered as Simulation A01 in this paper. The ultimate load level of Simulation A01 is 479 kN, which is similar to the simulation with the Shima bond-slip model and – more important – still a reasonable estimation. The corresponding crack pattern is given in figure 5. As a standard approach in ATENA, a fixed smeared crack

330 model with a crack width based shear retention factor is used in the simulation. Besides, when the predefined
 331 convergence criterion is not reached within 50 iterations, the program accept a relaxed convergence criterion.
 332 The crack patterns of the specimen before and after the peak load are indicated in Figure 5. With the fixed
 333 crack model, the crack pattern does not change with the change of the principal stress direction, thus a
 334 realistic flexural shear crack can be simulated as shown in Figure 5. In addition, in Simulation A01, it is possible
 335 to reach the descending branch of the load – deflection relations, see figure 6. That provides additional
 336 confidence of the simulations provided by DIANA, in which further loading were not possible. The crack
 337 pattern given by the simulations of ATENA compares well with the crack pattern after failure in figure 2. In
 338 ATENA, a realistic crack pattern is also found with a reference model with perfect bond. The simulation is not
 339 demonstrated in the paper.



341
 342 **Figure 5. Crack pattern (crack width > 0.01 mm) and horizontal strains in ATENA simulation (Simulation A01) with**
 343 **MC2010 bond splitting model at ULS load level (top, 479 kN) and just after maximum load (bottom) (2D-model with**
 344 **100x100 mm quadratic elements, displacement control, Arc Length solution method).**



345
 346 **Figure 6. Load displacement diagrams of Simulation D07 with Shima bond slip model using DIANA and Simulation A01**
 347 **with MC2010 A01 bond-slip model using ATENA.**

348
 349 Based on the discussion above, Simulation D07 and Simulation A01 are chosen as the final representative
 350 models. Figure 6 shows the load-displacement diagram of both models and that from the experiment. The
 351 displacement shown in the figure is the maximum deflection under the loading point. The comparison shows
 352 that both Simulation D07 and A01 provide rather similar load-deflection relationship, and they compare well



353 with the experimental observation. The main difference lies in the stiffness, which can be attributed the long
354 term deformation of concrete during the loading process. Comparing the stiffness of the first branches in
355 Figure 6 shows a reduction with a factor 0.74 from simulation to the test (Yang, et al., 2021b) and 0.77 in the
356 second branches. In an experiment that takes several hours a certain amount of creep will occur, which can be
357 simulated with a lower elastic modulus. Similar observation has been reported in (Cervenka, et al., 2016).
358 Besides, the first cracking loads in the simulations are higher than that observed in the experiments. This could
359 partly relate to the same phenomenon. Under sustained loading a reduced tensile strength may be expected
360 with comparable deformation as suggested by (Rusch, 1960; Reinhardt & Cornelissen, 1985). In addition, the
361 variation in concrete strength may result in a lower fracturing load (Tran & Graubner, 2018).

362 Discussions and recommendations

363 In this study, the following steps are made to improve the simulation, which can be summarized as advices for
364 the engineering practice when dealing with similar simulations:

- 365 1. Evaluation of mesh dependency.
- 366 2. Introduction of a bond-slip model when crack propagation at the level of the longitudinal
367 reinforcement is critical to the failure.
- 368 3. Further refinement of solving strategy (for example, manual selection of control displacement in an
369 arc length analysis).
- 370 4. For better crack pattern adaption of fixed crack model.

371

372 In this paper it is shown that indeed the influence of the so called modelling choices that were previously
373 considered to be less important may affect the simulation results considerably in this special situation. It
374 shows the risk of using NLFEM when it is applied on modelling of structure members with large dimensions
375 and brittle failure mode. In addition to that, the proposed improvement steps, have shown to give a realistic
376 approach to further improvement of the simulations. With this approach, simulations with good agreement to
377 the experimental results can be obtained. Despite that, as the intension of the paper is not to provide a
378 systematic study on how to accurately perform non-linear simulation of the flexural shear behaviour of RC
379 beams, further studies on the effect of the following aspects remain open:

- 380 1. The effect of element size to the simulation of structural members with large dimensions.
381 As discussed earlier, the presented study shows a clear influence of element size on the simulation
382 results. However, an opposite conclusion from that reported in a previous study (Cervenka, et al.,
383 2016) was obtained. To get a clear picture on the influence of element size in shear simulations,
384 further study is still necessary.
- 385 2. The effect of the bond-slip model in the simulation.
386 In this study, better results were reported after the introduction of a bond-slip model. Further
387 validation is needed on the choice of bond-slip model and the robustness of the simulation when such
388 bond-slip model is introduced.
- 389 3. In the simulations, a dowel crack along the longitudinal reinforcement was often observed during the
390 propagation of the critical shear crack. As the embedded reinforcement is usually considered as bar
391 elements, the bending stiffness, which is considered as the reason of dowel cracking, cannot be
392 simulated with this element type. Introduction of a beam type reinforcement element may further
393 improve the simulation.

394 Conclusions

395 This paper presents a post-diction study on the shear failure of specimen H123, with the intention to provide a
396 simple stepwise approach to improve simulations including flexural shear failure. It is demonstrated that the
397 simulation of the experimental results of H123 can be improved by refining modelling choices. The study
398 provides a practical stepwise example starting with a basic model, proposed by RTD 1016-1. The following
399 conclusions can be drawn:

- 400 1. The influence of the element size on the model simulation turns out to be rather complicated. This
401 study yields a different conclusion than the earlier study reported by (Cervenka, et al., 2016). Further
402 study on this topic is still needed.

- 403 2. Both the total strain rotating crack model and the total strain fixed crack model may provide sufficient
 404 accuracy. However, the fixed crack model is able to provide a more realistic crack pattern.
- 405 3. For the simulation of the shear behaviour of RC members without stirrups, introduction of a bond-slip
 406 model may improve the simulation results. Within this study both the bond-slip model suggested in
 407 Model Code 2010 and the model proposed by Shima give predictions closer to the test results than
 408 simulations with perfect bond.
- 409 4. More beams without stirrups should be simulated to quantify the model uncertainty for NLFEM
 410 simulation on the shear behaviour of RC members.
- 411 5. The work presented in the paper can be interpreted as a warning for users of RTD 1016-1 in case of
 412 deep beams without shear reinforcement. The simulation of such type of structures turns out to be
 413 more sensitive to the choices of the modelling parameters than for other types of structures.

414 Acknowledgements

415 The authors would like to acknowledge the Dutch ministry of infrastructure and environment (Rijkswaterstaat)
 416 for financially support the experimental research program in which the test of H123 was included.

417 References

- 418 Červenka, J., Červenka, V. & Laserna, S., 2018. On crack band model in finite element analysis of
 419 concrete fracture in engineering practice. *Engineering Fracture Mechanics*, Volume 197, pp. 27-47.
- 420 Bažant, Z., Belytschko, T. & Chang, T., 1984. Continuum theory for strain-softening. *Journal of*
 421 *Engineering Mechanics*, 110(12).
- 422 Bažant, Z. & Oh, B., 1983. Crack band theory for fracture of concrete. *Materials and Structures*,
 423 16(94).
- 424 Belletti, B., den Uijl, J., Hendriks, M. & Damoni, C., 2010. *Developing Standardized Guidelines for a*
 425 *Safety Assessment of Shear-Critical RC Beams Based on Nonlinear Finite Element Modeling*.
 426 Washington, s.n.
- 427 CEN, 2005. *Eurocode 2: Design of Concrete Structures - Part 1-1 General Rules and Rules for*
 428 *Buildings. NEN-EN 1992-1-1*. s.l.:s.n.
- 429 Cervenka, V., Cervenka, J., Pukl, R. & Sajdlov, T., 2016. Prediction of shear failure of large beam
 430 based on fracture mechanics. *FraMCoS-9*.
- 431 Cervenka, V. & Jendele, L., 2009. *ATENA program documentation part 1: Theory*, Prague: Cervenka
 432 Consulting.
- 433 de Putter, A., 2020. *Towards a uniform and optimal approach for safe NLFEM of reinforced concrete*
 434 *beams: Quantification of the accuracy of multiple solution strategies using a large number of*
 435 *samples*, Delft: s.n.
- 436 DIANA FEA, 2020. *DIANA User's Manual (release 10.3)*, Delft: s.n.
- 437 Ensink, S. W. H., van der Veen, C. & de Boer, A., 2015. Shear or bending? Experimental results on
 438 large t-shaped prestressed concrete beams. *Proceedings of the 16th European bridge conference*.
- 439 fib task group 8.2, 2008. *Constitutive modelling of high strength/high performance concrete*, s.l.: fib.
- 440 fib, 2012. *Model Code for Concrete Structures 2010*. Lausanne: Ernst & Sohn.
- 441 Jendele, L. & Cervenka, J., 2006. Finite element modelling of reinforcement with bond. *Computers*
 442 *and Structures*, Volume 84, p. 1780–1791.
- 443 Lantsoght, E., de Boer, A., van der Veen, C. & Hordijk, D., 2019. Optimizing Finite Element Models for
 444 Concrete Bridge Assessment With Proof Load Testing. *Front. Built Environ.*, p.
 445 <https://doi.org/10.3389/fbuil.2019.00099>.
- 446 Reinhardt, H. & Cornelissen, H., 1985. Sustained tensile tests on concrete (in German);
 447 Zeitstandzugversuche an Beton. *Bauverlag Wiesbaden*, pp. 162-167.
- 448 Rijkswaterstaat, 2017a. *Guidelines for nonlinear finite element analysis of concrete structures. RTD*
 449 *1016-1*. s.l.:s.n.



- 450 Rijkswaterstaat, 2017b. *Validation of the Guidelines for Nonlinear Finite Element Analysis of Concrete*
451 *Structures - Part: Overview of results. RTD 1016-2*, s.l.: s.n.
- 452 Rijkswaterstaat, 2017c. *Validation of the guidelines for NLFEA of RC structures Part Reinforced*
453 *beams(RTD1016-3A), Prestressed beams(RTD1016-3B) and Slabs(RTD1016-3C)*, Delft: s.n.
- 454 Rots, J., 1989. Crack models for concrete: discrete or smeared? fixed, multi-directional or rotating?.
455 *Heron*, 34(1).
- 456 Rusch, H., 1960. Researches Toward a General Flexural Theory for Structural Concrete. *Journal of the*
457 *American concrete institute*, 57(1), pp. 1-26.
- 458 Shima, H., Chou, L.-L. & OKAMURA, H., 1987. Micro and Macro Models for Bond in Reinforced
459 Concrete. *Journal of the Faculty of Engineering*, 39(22).
- 460 Slobbe, A., Hendriks, M. A. & Rots, J., 2013. Systematic assessment of directional mesh bias with
461 periodic boundary conditions: applied to the crack band model. *Engineering Fracture Mechanics*,
462 Volume 109.
- 463 Tran, N. L. & Graubner, C.-A., 2018. Influence of material spatial variability on the shear strength of
464 concrete members without stirrups. *BETON-UND STAHLBETONBAU International Probabilistic*
465 *Workshop 2018*.
- 466 Verhoosel, C. V., Remmers, J. J. C. & Gutiérrez, M. A., 2008. A dissipation-based arc-length method
467 for robust simulation of brittle and ductile failure. *International journal for numerical methods in*
468 *engineering*.
- 469 Yang, Y., 2014. *Shear behaviour of reinforced concrete members without shear reinforcement*, Delft:
470 s.n.
- 471 Yang, Y., de Boer, A. & Hendriks, M., 2021b. *A contest on modelling shear behaviour of deep concrete*
472 *slab strips using non-linear FEM*. Lisbon, s.n.
- 473 Yang, Y., den Uijl, J. & Walraven, J., 2017. Shear Behavior of Reinforced Concrete Beams without
474 Transverse Reinforcement Based on Critical Shear Displacement. *Journal of Structural Engineering*,
475 143(1).
- 476 Yang, Y., Naaktgeboren, M. & van der Ham, H., 2021b. *Shear capacity of RC slab structures with low*
477 *reinforcement ratio - an experimental approach*. Lisbon, s.n.
- 478